A&A 509, A34 (2010)
DOI: 10.1051/0004-6361/200912244

Astronomy & Astrophysics

A statistical approach to radio emission from shell-type SNRs

I. Basic ideas, techniques, and first results

R. Bandiera[1] and O. Petruk[2]

[1] INAF - Osservatorio Astrofisico di Arcetri Largo E. Fermi 5, 50125 Firenze, Italy
e-mail: bandiera@arcetri.astro.it
[2] Institute for Applied Problems in Mechanics and Mathematics Naukova St. 3-b, Lviv 79060, Ukraine

Received 1 April 2009 / Accepted 22 September 2009

ABSTRACT

Context. Shell-type supernova remnants (SNRs) exhibit correlations between radio surface brightness, SNR diameter, and ambient medium density, that between the first two quantities being the well known Σ–D relation.
Aims. We investigate these correlations, to extract useful information about the typical evolutionary stage of radio SNRs, as well as to obtain insight into the origin of the relativistic electrons and magnetic fields responsible for the synchrotron emission observed in radio.
Methods. We propose a scenario, according to which the observed correlations are the combined effect of SNRs evolving in a wide range of ambient conditions, rather than the evolutionary track of a "typical" SNR. We then develop a parametric approach to interpret the statistical data, and apply it to the data sample previously published by Berkhuijsen, as well as to a sample of SNRs in the galaxy M 33.
Results. We find that SNRs cease to emit effectively in radio at a stage near the end of their Sedov evolution, and that models of synchrotron emission with constant efficiencies in particle acceleration and magnetic field amplification do not provide a close match to the data. We discuss the problem of the cumulative distribution in size, showing that the slope of this distribution does not relate to the expansion law of SNRs, as usually assumed, but only to the ambient density distribution. This solves a long-standing paradox: the almost linear cumulative distribution of SNRs led several authors to conclude that these SNRs are still in free expansion, which also implies very low ambient densities. Within this framework, we discuss the case of the starburst galaxy M 82.
Conclusions. Statistical properties of SNR samples may be used to shed light on both the physics of electron acceleration and the evolution of SNRs. More precise results could be obtained by combining data of several surveys of SNRs in nearby galaxies.

Key words. ISM: supernova remnants – methods: statistical – radiation mechanisms: non-thermal – acceleration of particles – galaxies: individual: M 33 – galaxies: individual: M 82

1. Introduction

Radio emission is a quite common property of shell-type supernova remnants (SNRs). The intensity of the (synchrotron) radio emission is related to the magnetic field strength and the amount of accelerated electrons. However, the mechanisms leading to both the magnetic field amplification and the electron injection at the SNR shock and their respective efficiencies remain poorly constrained. To investigate these processes observationally, there have been detailed studies, mostly in X-rays, of some selected SNRs (see e.g., Cassam-Chenaï et al. 2007; Cassam-Chenaï et al. 2008, and references therein). Relevant, complementary information should also be extracted from a statistical analysis of SNR data samples.

On the observational side, a well-known (even though not widely accepted) statistical relation is the so-called "Σ–D relation", namely the empirical correlation discovered between the SNR size (D) and its radio surface brightness (Σ). Various authors (e.g., Clark & Caswell 1976; Milne 1979; Caswell & Lerche 1979; Case & Bhattacharya 1998; Urošević et al. 2005) have investigated this correlation. Originally applied as a tool for estimating SNR distances, it has been found to be unreliable for this purpose. Some authors (e.g., Green 2005; Urošević et al. 2005) have also argued that this correlation may be affected by selection effects. For Galactic SNRs, Green (2005) highlighted the selection effects: (1) in the surface brightness, with a completeness limit of about 10^{-20} W m^{-2} Hz^{-1} sr^{-1}, while SNRs below this limit are predominantly in regions where the Galactic background is low; (2) in the angular size, so that young but distant SNRs may be missed. For SNRs in other galaxies, Urošević et al. (2005) also showed that there may be a selection effect in the integrated flux (valid for unresolved or mildly resolved SNRs), with the effect of leading to an observed slope shallower than the intrinsic one.

Even though selection effects may affect this correlation to some level, we believe that the relation itself has a physical origin, and that one can therefore extract from it information about the processes involved in the SNR radio emission: therefore, understanding its origin could eventually contribute to constraining the efficiency of these processes. There have been several attempts (e.g., Shklovsky 1960; Van der Laan 1962; Poveda & Woltjer 1968; Kesteven 1968, or more recently Duric & Seaquist 1986; Berezhko & Völk 2004) to explain the Σ–D relation as the average evolutionary track of a "typical" SNR. In all of these cases, the slope of the correlation is assumed to correspond to that of the SNR evolutionary track on the Σ–D parameter plane.

However, there is clear evidence that this assumption is incorrect. Berkhuijsen (1986) has found tight correlations of

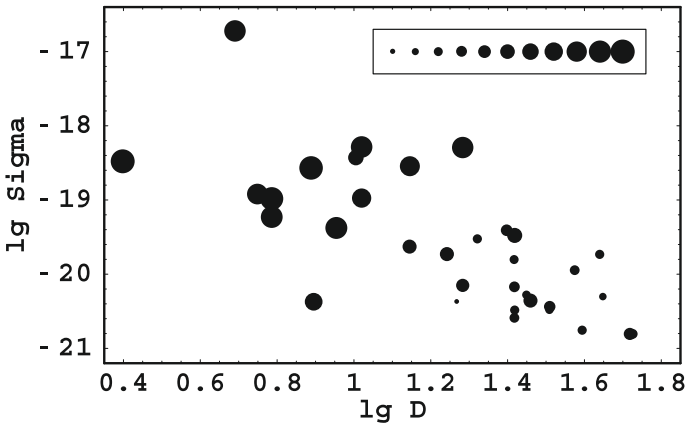

Fig. 1. Distribution of SNRs from Berkhuijsen (1986) sample in the $\lg D$–$\lg \Sigma$ parameter plane (D is measured in pc, while Σ is in $\mathrm{W\,m^{-2}\,Hz^{-1}\,sr^{-1}}$). The dot sizes are proportional to $\lg n_\mathrm{o}$ values, the legend showing in order sizes corresponding to $\lg n_\mathrm{o}$ from –1.5 to 1.0, in steps of 0.25 (n_o being measured in $\mathrm{cm^{-3}}$). It is apparent from this figure that smaller (and brighter) SNRs are typically located in a denser medium.

both Σ and D with the ambient density (n_o), in the sense that smaller (and brighter) SNRs are typically located in a denser medium (indeed, the correlation between n_o and D had already been known for several years; see e.g., Fig. 4 in McKee & Ostriker 1977). The best-fit results given by Berkhuijsen are

$$D \simeq 15\, n_\mathrm{o}^{-0.39\pm0.04}\ \mathrm{pc} \quad (1)$$

$$\Sigma \simeq 6\times10^{-20} n_\mathrm{o}^{1.37\pm0.21}\ \mathrm{W\,m^{-2}\,Hz^{-1}\,sr^{-1}}. \quad (2)$$

Berkhuijsen concluded that the Σ–D relation ($\Sigma \propto D^{\xi}$) is just a secondary effect, while the two primary relations are those of D and Σ with n_o.

Although this conclusion may appear rather extreme, it is quite obvious that the Σ–D relation contains SNRs that evolve in very different ambient conditions. We then assume that the correlations between Σ, D, and n_o do not directly reflect the evolution of a "typical" object, but are rather the combined effect of the evolution of different SNRs expanding in different ambient conditions. That the correlations with n_o are statistically so tight also suggests that D and Σ are more sensitive to the ambient conditions than to the SNR evolution. The combined effect of these correlations is that a clear trend of n_o across the Σ–D relation is observed (see Fig. 1), namely that smaller SNRs are preferentially located in higher-density environments.

In principle, correlations of Σ and D with n_o, accounting for at least qualitatively the trend of n_o across Σ–D relation, could also appear in the case of the evolution of an individual object, provided that it expands in a medium with a highly structured, fractal, density distribution. This would reflect that, during its life, a SNR always preferentially expands towards the direction in which the ambient density is lower. Therefore, at any time, the "effective" ambient density would be close to the "lowest" ambient density in the volume occupied by the SNR. In this way, one could explain why large SNRs typically seem to expand in a low-density medium.

However, it is hard to justify, in this scenario, the absence of small SNRs in low-density media (which would be the case, when the supernova itself is located in a low density region), as well as that low ambient density values are measured for all extended SNRs (which requires that such low density regions are ubiquitous in the Galaxy, on scales of tens of parsecs or even less). In addition, if the effects of the fractal interstellar medium were dominant, virtually all SNRs should have a much brighter limb on one side, which is not observed. Therefore, for all these reasons, we conclude that the "fractal ambient density" hypothesis is implausible, and we do not consider it any longer in this paper.

One of our goals is to show that the best-fit line usually referred to as the "Σ–D relation" provides only a minor part of the information present in the data, while additional information could be extracted by analyzing in detail the distribution of points in the Σ–D–n_o parameter space. For this reason we propose a rather general (parametric) scenario, with the aim of constraining the physics of the electron injection and magnetic field behavior in SNR shocks and/or the SNR evolutionary phase in which they are most likely to be observed in radio.

The plan of the paper is the following. In Sect. 2, we present the basic ideas, assumptions and formulae that will be used in the rest of the paper. Section 3 is devoted to a re-analysis of the data of Berkhuijsen (1986), using the criteria introduced in Sect. 2, and extracting constraints on the dependence of the particle and magnetic field efficiencies on the basic shock parameters. For the sake of comparison, we also apply the same technique to a sample of SNRs in galaxy M 33. Section 4 shows how the cumulative distribution of SNRs with diameter may be interpreted within our framework, and how we can explain the puzzling linear trend of this distribution without requiring, as usually done, that SNRs expand linearly to large sizes. Section 5 presents our conclusions.

2. Basic ideas, assumptions, and formulae

Our analysis is based on the fundamental criterion that the observed correlation in the Σ–D parameter plane originates from the combined effect of evolutionary tracks in very different ambient conditions. In this section, we implement this idea by adding some derived/secondary assumptions that will allow us to develop a more general scenario, on which our subsequent statistical analyses will be based.

2.1. When radio SNRs are preferentially seen

A preliminary consideration is that the conditions in which a given object is most likely observed, during its evolution, are those in which it spends most of its time. Since SNR expansion decelerates during most of their lifetime, it is statistically more likely to find them when their size is close to its final value. We are interested in finding SNRs that are visible in radio. Therefore, it is more important, in this case, to determine the evolutionary stage at which the processes responsible for enhancing magnetic fields and/or for producing high energy electrons are no longer efficient. In the following, we refer to this phase as the "final stage" of a radio SNR, but it should be clear that it is not the maximum size that a SNR can reach dynamically, before merging into the ambient medium.

We parametrize the SNR expansion by a power law ($D \propto t^{1/a}$; $a > 1$) up to a maximum size (D_2) beyond which the SNR is no longer detectable in radio. During its evolution of a given SNR as a radio source, the probability of being observed with a given size D is proportional to $\mathrm{d}t/\mathrm{d}D$, namely

$$\mathcal{P}(D) = aD^{a-1}/D_2^a, \quad \text{where} \quad D < D_2, \quad (3)$$

(the initial diameter of this evolutionary phase, D_1, not being relevant provided that $(D_1/D_2)^{a-1} \ll 1$), so that the average value

and standard deviation of the (decimal) logarithm of D are

$$\langle \lg D \rangle = \lg D_2 - \frac{1}{a \ln 10}, \quad (4)$$

$$\sigma_{\lg D} = \frac{1}{a \ln 10}. \quad (5)$$

For instance, during the adiabatic (Sedov) phase $a = 5/2$, so that $\langle \lg D \rangle = \lg D_2 - 0.17$ and $\sigma_{\lg D} = 0.17$, while, in the later radiative (pressure-driven snowplow) phase, $a = 7/2$, so that $\langle \lg D \rangle = \lg D_2 - 0.12$ and $\sigma_{\lg D} = 0.12$. This means that, on average, SNR diameters should be rather close to D_2, and that their dispersion should be rather small, i.e., an individual SNR, during its evolution, is seen to migrate only slightly in the Σ–D parameter plane. For this reason, we propose that selection effects, while important to determining the overall distribution of points across the Σ–D plane, should only have a marginal effect on the observed probability $\mathcal{P}(D)$.

2.2. The end of the radio phase

We consider, in particular, the end of the Sedov phase. According to Truelove & McKee (1999), it should correspond to a size

$$D_B \sim 28 \left(E_{\rm SN}/10^{51}\,{\rm erg}\right)^{2/7} n_{\rm o}^{-3/7}\,{\rm pc}, \quad (6)$$

(where $E_{\rm SN}$ is the energy of the supernova explosion), while the dynamical end of the SNR, namely where it merges with the ambient medium, can be placed at much larger sizes. The above formula has been obtained by approximating the plasma cooling function with a power law $\Lambda \propto T^{-1/2}$, where T is the gas temperature (while other papers use different power-law approximations; for instance, Blondin et al. 1998, use $\Lambda \propto T^{-1}$). For a generic $\Lambda \propto T^{-\alpha}$ relation one may find that

$$D_B \propto E_{\rm SN}^{(3+2\alpha)/(11+6\alpha)} n_{\rm o}^{-(5+2\alpha)/(11+6\alpha)}. \quad (7)$$

For α changing from 1/2 to 1, the exponent of $n_{\rm o}$ in the above formula changes from 0.429 to 0.412: namely, the numerical value of that exponent is very weakly dependent on the power-law approximation used. In the following, we shall then use, without loss of generality, the formula (here Eq. (6)) of Truelove & McKee (1999).

The correlation found by Berkhuijsen between D and $n_{\rm o}$ (Eq. (1)) is consistent with

$$D \simeq 0.54 \left(E_{\rm SN}/10^{51}\,{\rm erg}\right)^{-2/7} D_B, \quad (8)$$

namely with a D/D_B ratio that is independent of $n_{\rm o}$.

This can be also seen from Fig. 2, where the data points from Berkhuijsen (1986) are displayed together with D_B, as evaluated for $E_{\rm SN} = 10^{51}$ erg (solid line): we note that the line is not a fit, namely there are no free parameters to tune. This indicates that most of the known radio SNRs are observed close to the end of the Sedov phase, and that in general SNRs must extinguish their radio emission somewhere close to the end of their Sedov phase. It is then reasonable to use a Sedov law ($a = 5/2$) to approximate the expansion law during the final phases of radio SNRs: therefore, in the following, whenever a numerical value for a is required, we shall use the Sedov value. For a Sedov expansion, the dashed line in Fig. 2 applies to the value of $\langle \lg D \rangle$, given by Eq. (4) with $D_2 = D_B$. The best-fit level (Eq. (8)) is only 20% lower, providing a good argument for SNRs being (statistically) mostly visible around the end of their adiabatic stage.

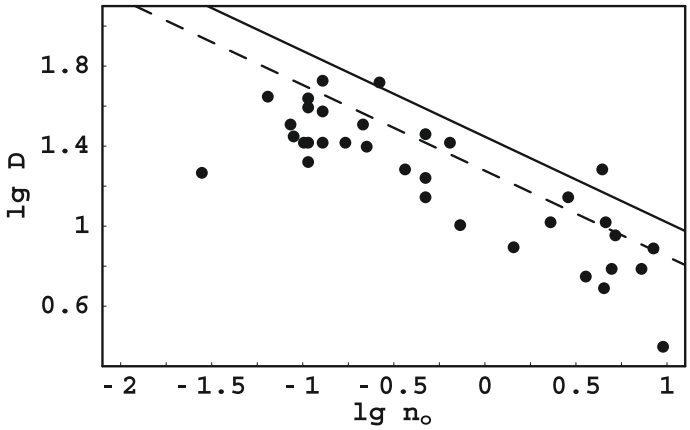

Fig. 2. Distribution of SNRs (from Berkhuijsen 1986 sample) in the $\lg n_{\rm o}$–$\lg D$ parameter plane. For comparison, the theoretical line corresponding to the end of the Sedov phase (as from Truelove & McKee 1999) is shown (solid line), as well as that of $\langle \lg D \rangle$, as from Eq. (4) (dashed line).

It remains to be understood for which physical reason the end of the Sedov phase should roughly correspond to the switching off of the radio emission. There is also evidence that the extinguishing transient evolution must be rather rapid. Otherwise, we should also see SNRs with Σ values considerably lower than that derived from the Σ–D correlation for the same size; namely, in the Σ–D parameter plane, we should have points spread over the half-plane below the main correlation (of course, limited to the region of the Σ–D plane for which one expects SNRs to be detectable). This latter piece of observational evidence is also not easy to explain. The underlying problem is that the physical processes behind the injection of electrons are poorly understood in the general case, and are probably even harder to model for conditions near to marginal efficiency.

2.3. The "final-stage" approximation

We introduce in a parametric form a basic set of equations to describe the observed correlations and distributions, and eventually provide some constraints on future physical models of the injection of electrons in SNRs. That the Σ–D empirical relation is a power law suggests (even though it does not strictly imply) that all formulae of interest can be approximated by power laws, thus simplifying considerably the treatment.

As a starting point, we consider the extreme approximation that each of them is observed very close to its final stage as a radio SNR, namely that each individual evolutionary track in the Σ–D plane can be assimilated to just one point, corresponding to its final position (D_2, Σ_2). We also assume that the dependence of both quantities on the ambient density ($n_{\rm o}$) can be approximated by the following power laws:

$$D_2(n_{\rm o}) = K_1 n_{\rm o}^m, \quad (9)$$

$$\Sigma_2(n_{\rm o}) = K_2 n_{\rm o}^n. \quad (10)$$

In this limiting case, the slope of the Σ–D relation

$$\Sigma_2(D_2) = K_3 D_2^{\xi}, \quad (11)$$

would simply be $\xi = n/m$. In the above formulae, the functional dependence on other physical parameters is not given explicitely; however, other quantities may be involved. For instance, if SNRs really are efficient radio emitters only until the

end of the Sedov phase (as suggested by Fig. 2), D_2 should also depend on the SN energy (see Eq. (7)).

To describe the distribution of points along the correlation, one must also introduce the function $\tilde{\mathcal{P}}(n_o)$, giving the probability of finding a SNR in a region of a given density: this probability combines the density distribution of the interstellar medium, the dependence of the SN rate on the local density, and how the lifetime of a radio SNR depends on the ambient conditions. For the sake of simplicity, and in the absence of any observational evidence against it, we also approximate this function by a power law, namely

$$\tilde{\mathcal{P}}(n_o) = K_4 n_o^w. \tag{12}$$

This distribution is used in Sect. 5.1.

2.4. Introducing the SNR evolution

From this point on, we shall remove the "final-stage" approximation, introduced in the previous section. Nonetheless the evolution of individual SNRs will still be treated in a very simplified way, by assuming that SNR evolution in different ambient conditions differ only by a scaling law and, in practice, by only adopting power-law behaviors.

We introduce the SNR expansion in the following parametric form:

$$t(D, n_o) = K_5 D^a n_o^b \tag{13}$$

(for instance, in the Sedov case $a = 5/2$, $b = 1/2$, and $K_5 \propto E_{SN}^{-1/2}$). As for the evolution in surface brightness, by assuming that a scaling law holds, the surface brightness could be expressed in a rather general form as

$$\Sigma(D, n_o) = f(D/D_2(n_o))\Sigma_2(n_o), \tag{14}$$

where $f(x)$ must vanish at $x > 1$. In this paper, we use a power-law approximation

$$\Sigma(D, n_o) = \left(\frac{D}{D_2(n_o)}\right)^p \Sigma_2(n_o) = K_6 D^p n_o^q \quad \text{for} \quad D < D_2, \tag{15}$$

where $K_6 = K_2/K_1^p$ and $q = n - mp$. Parameters p and q in Eq. (15) can be derived independently. If the data sample is not heavily affected by selection effects, these parameters can be evaluated by simply applying a bilinear regression.

Determining the functional dependence of $\Sigma(D, n_o)$ would also allow one to derive the trajectory of individual SNRs in the parameter plane. They are simply given by the function $\Sigma(D)$ for a constant value of n_o, which in principle differs from the $\Sigma(D)$ relation, as traditionally obtained, because the latter relation is obtained by combining cases with different n_o values. In the power-law case, the slope of the evolutionary track of an individual SNR is then given by the exponent p. In the following, we shall provide some evidence that the value of p is different from that of ξ: this means that evolutionary tracks in the Σ–D parameter plane have a different slope from that of the overall Σ–D relation.

Also m can be derived, by fitting Eq. (9) to the D–n_o data (provided that $\langle D \rangle$ is a constant fraction of D_2, as from Eq. (4)). On the other hand, there is no way of deriving a and b (defined in Eq. (13)) directly from the correlations between Σ, D, and n_o. Coefficient a could be inferred, in principle, only by studying the distribution of points about the main correlation (a point that will be treated in a forthcoming paper), while there is no way of estimatig the exponent b, because it would only affect the distribution of points with n_o along the correlations, a piece of information that is already included in the definition of the distribution $\tilde{\mathcal{P}}$ (Eq. (12)).

In principle, a distribution of SN energies may also contribute; but, for the present analysis, we assume that SN energies are not correlated with any other quantity and therefore that a distribution of energies would just produce an additional dispersion across the correlations, without affecting any of the above slopes. Some correlation could be possible, in principle, if different population stars have different distributions of their SN energies. However, to our knowledge no evidence in favour of this has been presented so far.

3. Statistical analysis of the data

3.1. Data sample and best-fit parameters

We now apply the analysis outlined above to the data published by Berkhuijsen (1986). That paper presents a fundamental work on the subject and, although since then a great number of surveys of higher accuracy have been performed, it still contains the most extended data sample of SNRs in which, in addition to the SNR radio surface brightness and size, quantities derived by other spectral bands are also tabulated. We extracted from this data sample all SNRs with available data on Σ, D (radio), and n_o as well. We excluded SN 1006, because it is now known that the bulk of its X-ray emission is non-thermal. The total number of selected objects is 34: the original data sample is given in Table 1 (for two objects, Cas A and Tycho, in which two different values of n_o are given, we took their geometrical mean). Since distance estimates for Galactic SNRs have changed with time, in the last column of Table 1 we list the SNR sizes obtained from the most recent version of the Galactic SNR catalog, by Green (2009): they differ substantially from Berkhuijsen's values only for Kepler and Vela. The estimated distances of the Large Magellanic Cloud (LMC) and the Small Magellanic Cloud (SMC) have also slightly changed, from 55 kpc and 63 kpc (as in Berkhuijsen 1986), to 48 kpc and 61 kpc (Macri et al. 2006, Hilditch et al. 2005), respectively. In our calculations, we used all of these new distances, and we revised accordingly the SNR linear size and density estimates (being $n_o \propto d^{-1/2}$). The last two columns of Table 1 provide the D and n_o values that we used.

The average ambient density is estimated by Berkhuijsen (1986) in a simple way, using the following relation (derived from Long 1983):

$$n_o = (6/\pi)^{1/2} \epsilon^{-1/2} f^{1/2} L_X^{1/2} D^{-3/2}, \tag{16}$$

where ϵ (taken to be 3×10^{-23} erg cm^{-3} s^{-1}) is the specific emissivity, f is the filling factor (taken to be close to unity), and L_X is the X-ray luminosity. While the exact values of ϵ and f are not important to our statistical analysis, it is crucial that these quantities remain constant, or at least independent of other parameters (such as size and surface brightness). In spite of its simplicity, this formula provides reasonably good results. Upper limits to the uncertainty in this n_o evaluation can be derived from the dispersion about the $\lg D$–$\lg n_o$ regression. Based on the assumption that the measured dispersion depends only on the uncertainties in n_o, one obtains $\sigma(\lg n_o) = 0.42$; while also taking into account the dispersion in D, as modeled by Eq. (5) for the case of Sedov expansion, one derives a residual dispersion $\sigma(\lg n_o) = 0.18$, namely a typical uncertainty in the density derived by Berkhuijsen of only about 50%.

Table 1. The data sample (extracted from Berkhuijsen 1986).

	Object	$-\lg\Sigma$ (W m^{-2} Hz^{-1}sr^{-1})	D (as from Berkhuijsen) (pc)	n_o (cm^{-3})	D (after distance revision) (pc)	n_o (cm^{-3})
GAL	W44	19.409	26.0	0.22	25.0	0.22
GAL	Cas A	16.721	4.1	4.94	4.9	4.52
GAL	Tycho	18.921	5.4	3.64	5.6	3.57
GAL	RCW103	19.377	9.6	5.04	9.0	5.21
GAL	Kepler	18.481	3.8	7.70	2.5	9.49
GAL	W49B	18.432	11.0	0.70	10.1	0.73
GAL	VelaXYZ	20.367	36.0	0.02	18.5	0.03
GAL	RCW86	20.276	35.0	0.08	28.1	0.09
LMC	0453–685	19.730	20.0	0.44	17.5	0.47
LMC	0454–665	19.629	16.0	0.44	14.0	0.47
LMC	0455–687	20.299	51.0	0.06	44.5	0.06
LMC	0500–702	20.590	30.0	0.12	26.2	0.13
LMC	0505–679	20.374	9.0	1.34	7.9	1.43
LMC	0506–680	18.976	12.0	2.14	10.5	2.29
LMC	0509–675	19.231	7.0	4.64	6.1	4.97
LMC	0519–697	19.524	24.0	0.10	20.9	0.11
LMC	0519–690	18.984	7.0	6.76	6.1	7.24
LMC	0520–694	20.435	37.0	0.20	32.3	0.21
LMC	0525–660	19.480	30.0	0.60	26.2	0.64
LMC	0525–696	18.293	22.0	4.12	19.2	4.41
LMC	0525–661	18.544	16.0	2.68	14.0	2.87
LMC	0527–658	20.807	61.0	0.12	53.2	0.13
LMC	0528–692	20.168	30.0	0.16	26.2	0.17
LMC	0532–710	19.947	43.0	0.12	37.5	0.13
LMC	0534–699	20.356	33.0	0.44	28.8	0.47
LMC	0534–705	20.481	37.0	0.08	32.3	0.09
LMC	0535–660	18.287	12.0	4.30	10.5	4.60
LMC	0536–706	20.481	30.0	0.10	26.2	0.11
LMC	0543–689	20.758	45.0	0.10	39.3	0.11
LMC	0547–697	19.736	50.0	0.10	43.6	0.11
LMC	0548–704	20.151	22.0	0.34	19.2	0.36
SMC	0045–734	19.802	27.0	0.10	26.1	0.10
SMC	0102–722	18.570	8.0	8.28	7.7	8.41
SMC	0103–726	20.807	54.0	0.26	52.3	0.26

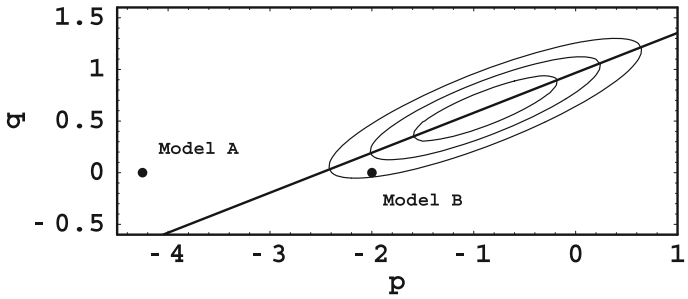

Fig. 3. Plot of the confidence levels in the $p-q$ parameter plane. The levels plotted correspond to 1, 2, and 3-σ confidence levels, while the line indicates the maximum spread direction (see Eq. (21)). For comparison, two theoretical predictions are plotted: "Model A" $(-17/4, 0)$ indicates the case with constant efficiency in both particle acceleration and magnetic field compression plus amplification (Berezhko & Völk 2004); while "Model B" $(-2, 0)$ refers to the case in which particles are accelerated with constant efficiency but the magnetic field is constant (see text).

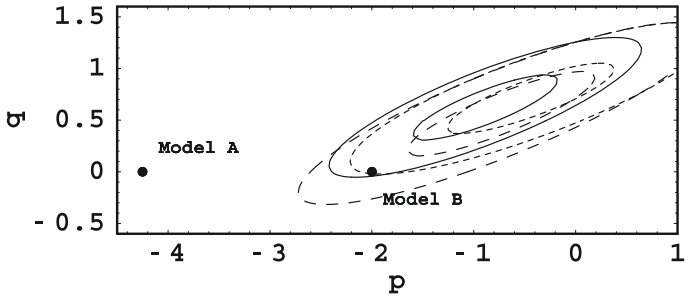

Fig. 4. Plot of the 1-σ and 3-σ confidence levels in the $p-q$ parameter plane, for the whole sample (solid lines), as well as for selections of the 25 and 30 SNRs with the highest surface brightness (short-dashed and long-dashed lines, respectively).

By performing linear regressions between the logarithmic quantities (which is equivalent to assuming constant relative errors in the measurements), we obtain:

$$m = -0.37 \pm 0.04, \quad (17)$$

$$\xi = -2.06 \pm 0.34, \quad (18)$$

$$p = -0.89 \pm 0.57, \quad (19)$$

$$q = +0.62 \pm 0.25, \quad (20)$$

(where 1-σ uncertainties are indicated). It is apparent that, while m and ξ are found to have reasonably small uncertainties, the uncertainties of p and q are larger. The reason is that, in the data, there is a near-degeneracy between p and q, as is well shown by a plot of the confidence levels (Fig. 3). In this sense, a combined quantity that can be far more reliably determined is:

$$q - 0.39p = 0.97 \pm 0.14. \quad (21)$$

A potential problem of this sample, and of SNR samples in general, is the presence of selection effects. In the introduction, we mentioned the analyses of Green (2005) and Urošević et al. (2005) on this subject. The points raised by Green (2005) are more appropriate to our sample, which consists only of SNRs located in our Galaxy and the Magellanic Clouds.

Even though a detailed treatment of the selection effects is beyond the scope of this paper (but will be approached in a forthcoming paper), for the sake of illustration we repeated the computations that led to Fig. 3, but on subsamples containing, respectively, the 25 and 30 SNRs with the highest radio surface brightness with corresponding thresholds in $\lg\Sigma$ of -20.356 and -20.481 respectively (see Table 1). Figure 4 shows a comparison of the confidence levels (only 1-σ and 3–σ, for figure clarity) for the two subsamples, superimposed on those for the entire sample (as in Fig. 3). It is apparent that any additional selection in surface brightness does not generate any substantial difference in the results, apart from a slight terms of broadening compatible with the lower sample size being analyzed by statistics and a slight shift toward lower p and q values (the latter point will be discussed in the next section).

3.2. Testing the "constant efficiencies" model

Among the various theoretical attempts to model the radio emission from SNRs, one of the most recent and popular is that by Berezhko & Völk (2004). This paper assumes that the kinetic energy density entering the shock ($mn_o V_{sh}^2$, where m is the mean atomic mass) is converted with constant efficiencies into the energy densities of magnetic field and accelerated electrons (ϵ_B and ϵ_{CR}, respectively): this means, for instance, that the effective magnetic field in the synchrotron emitting region decreases with time, simply because the SNR shock is slowing down. For

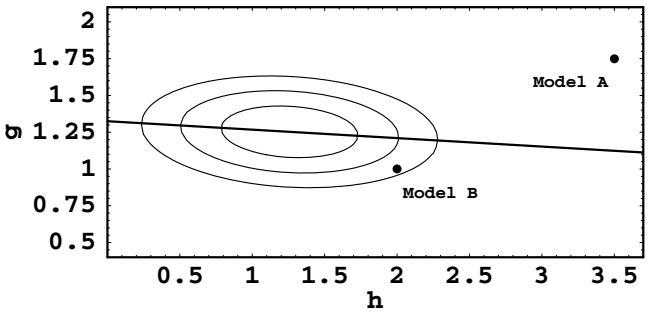

Fig. 5. Same as Fig. 3, in the $g - h$ parameter plane.

synchrotron emission with a power index −0.5 (namely the average index for radio SNRs), the surface brightness should scale as

$$\Sigma \propto KB^{3/2}D \propto \left(\epsilon_{\rm CR}\epsilon_B^{3/4}\right) D \propto \left(n_{\rm o}V_{\rm sh}^2\right)^{7/4} D. \quad (22)$$

A further assumption of this model is Sedov expansion, which implies that $mn_{\rm o}V_{\rm sh}^2 \sim E_{\rm SN}/D^3$, so that one finally obtains

$$\Sigma \propto E_{\rm SN}^{7/4}D^{-17/4}, \quad (23)$$

i.e., with $p = -4.25$, and $q = 0$ (labeled as "Model A" in Fig. 3). Namely, according to this model, individual SNR tracks in the Σ–D plane must be rather steep and "independent of the ambient density". Since Berezhko & Völk (2004) state that the slope of the Σ–D relation should represent the slope of individual evolutionary tracks, they predict that $\xi = -4.25$ should be the slope of the Σ–D relation. However, neither their predicted value for ξ matches the data, nor does (and at an even higher significance level) their predicted (p, q) pair (see Fig. 3). It is unlikely that this mismatch is a mere consequence of a sample incompleteness in surface brightness. Figure 4 shows that for subsamples in which a further selection in surface brightness has been applied the barycenter of the confidence levels moves only mildly.

A more appropriate model (in the sense that it is "only" about 2-σ away from the best-fit model values) would be one in which electrons are accelerated with constant efficiency ($\epsilon_{\rm CR} \propto n_{\rm o}V_{\rm sh}^2$) but the magnetic field is taken to be constant, not only during the evolution of an individual SNR but also among different SNRs. This happens, for instance, if the post-shock field has been compressed only by the shock, i.e., is proportional to the ambient field, which in turn is roughly constant (see e.g., Crutcher et al. 2003), in near equipartition with the interstellar thermal pressure of the diffuse interstellar medium. This case does not exclude the presence of an extra field amplification, provided that it yields a constant factor. As in the previous case, but assuming B to be constant, one can now write

$$\Sigma \propto KD \propto \epsilon_{\rm CR}D \propto \left(n_{\rm o}V_{\rm sh}^2\right) D \propto E_{\rm SN}D^{-2}, \quad (24)$$

namely $p = -2$ and $q = 0$ (which is labeled "Model B" in Fig. 3).

3.3. The results with a more "physical" flavour

We can approach the problem from the opposite direction, by trying to translate the information derived in terms of (p, q) into constraints on the physics that controls the magnetic and cosmic-ray efficiencies. We assume that

$$KB^{3/2} \propto n_{\rm o}^g V_{\rm sh}^h, \quad (25)$$

where g and h are free parameters. This is not the most general case, but it simply relates the efficiencies to primary local quantities encountered by the shock. Based on this assumption, and an expansion law $t \propto D^a$ passing through the endpoint of the Sedov phase (D_B, t_B), the equation for the surface brightness becomes

$$\Sigma \propto E_{\rm SN}^{(4a-3)/14} D^{1-(a-1)h} n_{\rm o}^{g-(3a-4)h/7}. \quad (26)$$

In the case of Sedov expansion, this equation simplifies into

$$\Sigma \propto E_{\rm SN}^{1/2} D^{1-3h/2} n_{\rm o}^{g-h/2}. \quad (27)$$

Figure 5 shows the confidence levels in this new pair of parameters. An advantage is that the direction of maximum dispersion is almost parallel to the h axis, which means that at least the best-fit value for g is well determined. We have

$$g = 1.25 \pm 0.14, \quad (28)$$

$$h = 1.26 \pm 0.38. \quad (29)$$

For comparison, the "constant efficiencies" model prescribes that $g = 1.75$ and $h = 3.5$, as can easily be derived from Eqs. (23) and (27). What we have found here is not different from the previous section, but is simply displayed in a more physical way.

To summarize, in most SNRs the constant efficiency assumption (namely for both field amplification and particle acceleration) does not hold. This may not be surprising, in the view that the statistically most common cases are those of SNRs close to their radio endpoint, namely when particle acceleration is close to being halted. Using observations to test these critical cases may indeed be important to obtaining a clearer understanding of the physical processes responsible for magnetic amplification and particle acceleration.

4. Results from an independent sample: M 33

As already mentioned in the introduction, SNR samples studied in other galaxies provide promising input to this kind of analysis. On the other hand, the presence of selection effects could affect the results (Urošević et al. 2005), and a statistical analysis of these samples should include a careful study of these. Extragalactic SNR samples will be considered in more detail in a forthcoming paper. For mere comparison with what has already been obtained using the sample of Berkhuijsen, we present here the results for a M 33 SNR data sample, which is a sample completely independent from that used so far.

The sample was obtained by selecting SNRs for which radio fluxes are given by Gordon et al. (1999), X-ray fluxes by Pietsch et al. (2004), and (optical) diameters by Gordon et al. (1998). The X-ray survey of Plucinsky et al. (2008), based on Chandra data, was also used to solve some cases of uncertain identification. In this way, we selected 22 SNRs: the data sample is shown in Table 2. The first 3 columns report the SNR identification numbers in the various catalogs, respectively, Gordon et al. (1998, labeled by "opt" in the table), Gordon et al. (1999, labeled by "rad"), and Pietsch et al. (2004; labeled by "xray"), while the next 3 columns show, respectively, the published linear (optical) diameters, 20 cm fluxes, and measured (i.e., absorbed) 0.2–4.5 keV fluxes.

To derive 1 GHz radio fluxes, we extrapolated the 20 cm fluxes tabulated by Gordon et al. (1999), by assuming a spectral index of −0.5. For most SNRs, Gordon et al. (1999) also estimate spectral indices, but the uncertainty in these estimates is rather large, and we therefore preferred to adopt a "standard" value for the spectral index. We evaluated the unabsorbed X-ray fluxes by taking a column density $N_{\rm H} = 1.0 \times 10^{21}\,{\rm cm}^{-2}$ towards M 33 (Plucinsky et al. 2008), and assuming for the average SNR spectrum a Raymond-Smith model with $kT = 0.3$ keV. Using

Table 2. M 33 data sample.

ID opt	ID rad	ID xray	D (pc)	S(20 cm) (mJy)	Flux(0.2–4.5) (erg cm^{-2} s^{-1})
9	11	93	18	0.7	4.29×10^{-15}
11	13	98	17	0.6	3.81×10^{-15}
15	20	106	27	0.6	2.79×10^{-15}
20	25	120	10	0.8	1.03×10^{-14}
21	29	121	28	0.9	1.41×10^{-13}
25	42	144	27	1.4	3.63×10^{-15}
27	47	153	23	1.2	2.99×10^{-15}
28	50	158	11	0.8	2.45×10^{-14}
29	52	161	20	0.5	1.73×10^{-14}
31	57	164	39	1.8	3.88×10^{-14}
35	64	179	32	3.5	1.01×10^{-14}
42	75	194	29	0.5	1.39×10^{-14}
47	90	207	36	0.2	7.05×10^{-15}
53	110	213	40	0.2	1.53×10^{-15}
54	111	214	16	1.3	2.08×10^{-15}
55	112	215	18	4.4	2.84×10^{-14}
57	114	220	21	0.4	1.87×10^{-15}
59	121	224	16	0.3	3.90×10^{-15}
62	125	225	29	0.4	4.87×10^{-15}
64	130	230	27	0.5	3.65×10^{-15}
73	148	250	17	0.5	1.41×10^{-14}
97	181	314	35	0.8	4.84×10^{-15}

WebPIMMS[1], a correction factor of ∼1.94 is evaluated: the precise value of this factor is not very important for our purposes, provided that the X-ray SNR spectra are not too different among themselves. Finally, a M 33 distance of 817 kpc (Freedman et al. 2001) is assumed here; since Gordon et al. (1998) use a distance of 840 kpc, for consistency we applied a small correction to their published SNR sizes.

Here are our results, to be compared with those presented above. The formulae equivalent to Eqs. (17)–(20), (28) and (29) are respectively

$$m = -0.34 \pm 0.07, \quad (30)$$
$$\xi = -2.20 \pm 0.46, \quad (31)$$
$$p = -1.37 \pm 0.64, \quad (32)$$
$$q = +0.52 \pm 0.30, \quad (33)$$
$$q - 0.37p = 1.04 \pm 0.20 \quad (34)$$
$$g = 1.31 \pm 0.20 \quad (35)$$
$$h = 1.58 \pm 0.42; \quad (36)$$

while Figs. 6–9 correspond, for M 33, to Figs. 1–3, and 5, respectively. It is apparent that all results from this further sample show close agreement, within the quoted errors, with what we found above using the data of Berkhuijsen. A comparison of the regression results for the two samples is given in Table 3.

5. The SNR cumulative distribution with size

5.1. The original paradox and how it can be solved

The cumulative distribution of the number of SNRs with sizes smaller than a given diameter (N–D relation) is another statistical distribution that has traditionally been studied.

For the Magellanic Clouds, Mills et al. (1979) derived an almost linear relation ($N \propto D^{1.2}$) up to sizes as large as 40 pc. They also argued that a similar relation should be present in our

[1] http://heasarc.gsfc.nasa.gov/Tools/w3pimms.html

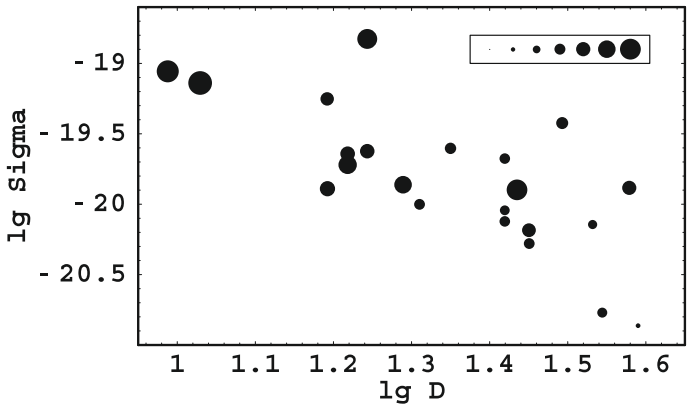

Fig. 6. Distribution of the M 33 SNRs sample in the lg D–lg Σ parameter plane (to be compared with Fig. 1). The dot sizes are proportional to lg n_o values, the legend showing in order sizes corresponding to lg n_o from –1.0 to 0.5, in steps of 0.25.

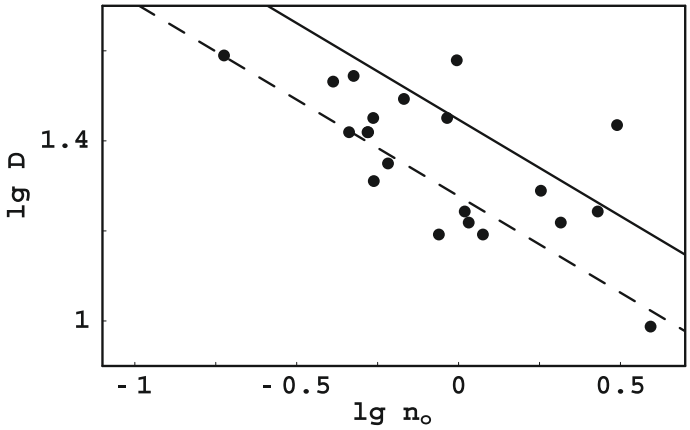

Fig. 7. Distribution of M 33 SNRs in the lg n_o–lg D parameter plane (to be compared with Fig. 2).

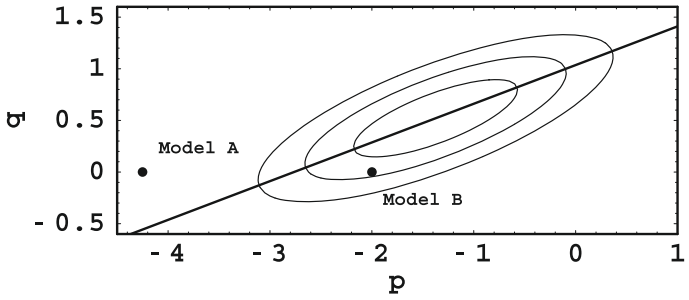

Fig. 8. Plot, for M 33 SNRs, of the confidence levels in the $p-q$ parameter plane (to be compared with Fig. 3).

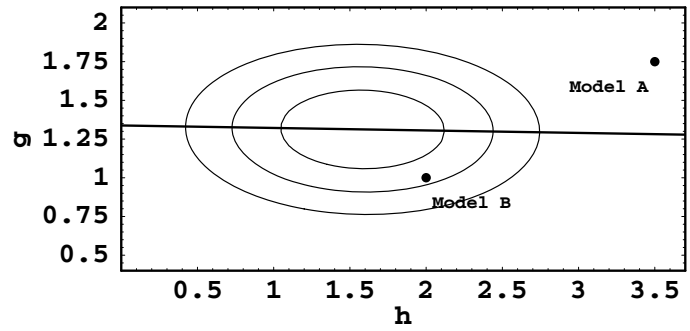

Fig. 9. Plot, for M 33 SNRs, of the confidence levels in the $g-h$ parameter plane (to be compared with Fig. 5).

Table 3. Synoptic table of the results of the regression analyses.

Formula		Data Samples	
		Berkhuijsen	M 33
$D_2(n_o) \propto n_o^m$	$m =$	-0.37 ± 0.04	-0.34 ± 0.07
$\Sigma_2(D_2) \propto D_2^{\xi}$	$\xi =$	-2.06 ± 0.34	-2.20 ± 0.46
$\Sigma(D, n_o) \propto D^p n_o^q$	$p =$	-0.89 ± 0.57	-1.37 ± 0.64
	$q =$	$+0.62 \pm 0.25$	$+0.52 \pm 0.30$
$q - \lambda p = \mu$	$\lambda =$	$+0.39$	$+0.37$
	$\mu =$	$+0.97 \pm 0.14$	$+1.04 \pm 0.20$
$KB^{3/2} \propto n_o^g V_{sh}^h$	$g =$	$+1.25 \pm 0.14$	$+1.31 \pm 0.20$
	$h =$	$+1.26 \pm 0.38$	$+1.58 \pm 0.42$

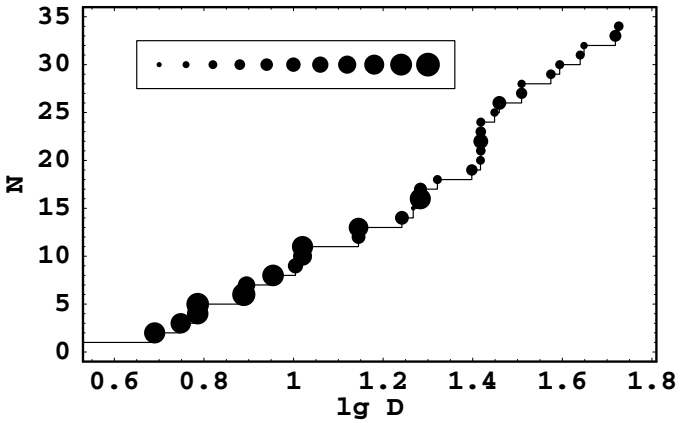

Fig. 10. Cumulative distribution, for Berkhuijsen's sample, where the dot sizes are proportional to the $\lg n_o$ value of the last SNR entering in the cumulative. The legenda uses for the dot sizes the same convention as in Fig. 1.

Galaxy. A linear cumulative distribution is usually taken as evidence that these SNRs are still in free expansion. However, when the SNR diameter is 40 pc, the swept-up mass is $\sim(1000/n_o)\,M_\odot$. Therefore, except for cases of exceptionally low ambient density, at those sizes SNRs should already be in the Sedov phase, and therefore strongly decelerated. A way to solve this paradox was suggested by Green (1984), which invokes a major effect of sample incompleteness. Indeed, any sample incompleteness is expected to substantially affect the cumulative distribution. Much less pronounced effects on the Σ–D correlation, as well as on the correlations discussed in Sect. 3, are expected, since the main effect of the sample incompleteness should be to change the distribution of points "along" the correlations. The relevance of data sample incompleteness to the correlations will be discussed in a forthcoming paper.

Within our framework, the cumulative distribution with size is independent of the expansion law of individual SNRs, but is related instead to the statistical distribution of the ambient medium density, as defined by Eq. (12). Indeed

$$N(D) \propto \tilde{\mathcal{P}}(n_o) n_o \propto D^{(1+w)/m}. \quad (37)$$

In this sense, it is not even necessary to account for the sample incompleteness, as done by Green (1984).

For the sake of illustration, Fig. 10 shows the $N(D)$ cumulative distribution of Berkhuijsen's sample. Here the close to linearity of the distribution is coincidental, since there is no reason to expect the sample of Berkhuijsen to be complete. Instead, the trend of dot sizes with SNR diameter (which is to some extent a different way of displaying the information contained in Fig. 2) clearly shows how, for increasing size, the cumulative is more and more populated by SNRs located in more tenuous ambient media.

5.2. The case of M 82

Samples of SNRs in nearby galaxies have become increasingly available, and the close to linearity of the N–D relation is a rather standard property of these samples.

A particularly interesting case is that of M 82. In this nearby starburst galaxy, a number of radio sources have been detected (Kronberg et al. 1985), which may be SNRs that are much brighter and much smaller in size (a few parsec at most) than usual. Their positions on the Σ–D parameter plane are in all cases consistent with the extrapolation to lower sizes of the best-fit Σ–D relation for other galaxies. Chevalier & Fransson (2001) proposed that these sources are SNRs expanding in a high-density ambient medium (with densities of order of 10^3 cm^{-3}).

Kronberg et al. (2000) also placed upper limits on the flux density variations in most of the radio sources: approximately 75% of these objects are very stable, with a lower limit of $\sim 10^3$ yr to their characteristic radio-emitting lifetimes. Based on this upper limit, Seaquist & Stankovic (2007) suggested that they may not be SNRs, but rather cluster wind-driven bubbles. Their main argument is that the lack of observed time variability is inconsistent with the estimated ages of these objects. That is, if they are SNRs in free expansion (with typical velocities of $\sim 10\,000$ km s^{-1}), their ages should be a few hundred years at most, while to account for the lack of variability, velocities no greater than ~ 500 km s^{-1} are required (Chevalier & Fransson 2001).

A crucial point in this reasoning is the expansion regime of these objects, if they are indeed SNRs. A linear expansion is argued by both Muxlow et al. (1994) and Fenech et al. (2008) based on the cumulative distribution with size being almost linear. However, as we have explained above, a linear cumulative distribution does not imply a linear expansion, if it is caused by the combination of SNRs expanding in different ambient densities. Indeed, the data for SNRs in M 82 agree well with the extrapolation of the Σ–D relation derived for SNRs in other galaxies to smaller sizes. Thus, the arguments we have exposed in this paper should also be applied to SNRs in M 82.

Even though they have small sizes in the parsec range (Muxlow et al. 1994), they could be close to the end of their Sedov phase provided that the ambient densities are $\sim 10^3$ cm^{-3}, with corresponding shock velocities of $\sim 10^3$ km s^{-1} compared to $\sim 10^4$ km s^{-1} as in the case of undecelerated expansion. These lower shock velocities infer characteristic times of $\sim 10^3$ yr, compatible with the average radio-emitting lifetime found by Kronberg et al. (2000). The only exceptions are a few fast-evolving radio sources that are probably radio SNe, namely young objects still evolving in their circumstellar medium. Although the detailed physical conditions and processes at such high densities may differ from those at densities typical of other galaxies, we are confident that the simple estimate presented above is adequate to justify the large measured characteristic times within our framework. Finally, Fenech et al. (2008) claimed to have measured very high expansion velocities, up to 10 000 km s^{-1}: these measurements seem to conflict not only with our model but also with the above-mentioned photometric measurements (Kronberg et al. 2000). Therefore, it is probably too early to discuss these latest measurements.

6. Conclusions

We have shown that studies of the statistical properties of SNR samples may provide insight into the physics of electron acceleration and the time evolution of SNRs. We have proposed a new scenario, along the lines of previous work by Berkhuijsen (1986), which interprets in a natural way the observed correlations between radio surface brightness Σ, size D, and ambient density n_o in a sample of SNRs. The main parameter of SNR evolution that enters into these correlations is the time at which a SNR ceases to behave as a radio source, and we find that this endpoint is located close to the end of the Sedov phase. We otherwise find that the observed correlations mostly reflect that the sample consists of SNRs located in very different ambient conditions; while the evolution of individual SNRs plays a secondary role, and cannot be extracted by simply studying correlations between pair of quantities.

Within this framework, we present a new approach to analyzing the statistical data, based on a 2-dimensional fit to Σ as a function of D and n_o. We show that the slope of $\Sigma(D)$ at constant n_o should represent more closely the true evolutionary track of an individual SNR than the well known "Σ–D relation", which is obtained without including information about n_o.

In this work, we have used data published by Berkhuijsen (1986). Although this data sample is rather limited, our method of analysis applied to these data is already capable of discriminating to some level between different theoretical models. For instance, models prescribing constant efficiencies for both magnetic field (turbulent) amplification and electron acceleration (e.g., Berezhko & Völk 2004) are well outside the parameters region allowed by the data. On the other hand, models assuming a constant acceleration efficiency but a constant post-shock magnetic field are marginally (about 2-σ) consistent with the data. For the sake of comparison, we have applied the same technique to a sample of SNRs in M 33. Although this sample could be affected by selection effects, it is completely independent from the sample of Berkhuijsen, and the parameters that we derive from the two samples are in close agreement, within the statistical errors. This may indicate again that our technique is robust andthe assumptions at the basis of our statistical analysis are correct. With the use of larger and more accurate data samples the confidence interval will become narrower, and the statistical results will be capable of constraining models more tightly.

In nearby galaxies, deep and detailed surveys of SNRs have become available in both radio and X-rays. The number of SNRs in other galaxies has increased considerably, with reasonably good radio and X-ray flux measurements and in various cases also information about their angular size. Although SNRs in external galaxies are more difficult objects to observe than Galactic SNRs, their distances are well known (since they correspond to the distance of the parent galaxy); in addition, selection effects can be modeled in a more accurate way for a sample of SNRs that are all at the same distance. Therefore, a natural extension of the present work is to elaborate our diagnostic tools along the guidelines shown in this paper, and to use them to investigate SNRs samples in various nearby galaxies. These results will be presented in a forthcoming paper.

Acknowledgements. O.P. acknowledges the hospitality of INAF - Osservatorio Astrofisico di Arcetri, where most of this work was carried out. R.B. acknowledges the hospitality of KITP, Santa Barbara, during the last phase of revision of the manuscript. This work was partially supported by the PRIN-MIUR 2006, by the ASI under Grant ASI-INAF No. I/023/05/0, and by the NSF under Grant No. PHY05–51164.

References

Berezhko, E. G., & Völk, H. J. 2004, A&A, 427, 525
Berkhuijsen, E. M. 1986, A&A, 166, 257
Blondin, J. M., Wright, E. B., Borkowski, K. J., & Reynolds, S. P. 1998, ApJ, 500, 342
Clark, D. H., & Caswell, J. L. 1976, MNRAS, 174, 274
Cassam-Chenaï, G., Hughes, J. P., Ballet, J., & Decourchelle, A. 2007, ApJ, 665, 315
Cassam-Chenaï, G., Hughes, J. P., Reynoso, E. M., Badenes, C., & Moffett, D. 2008, ApJ, 680, 1180
Case, G. L., & Bhattacharya, D. 1998, ApJ, 504, 761
Caswell, J. L., & Lerche, I. 1979, MNRAS, 187, 201
Chevalier, R. A., & Fransson, C. 2001, ApJ, 558, L27
Crutcher, R., Heiles, C., & Troland, T. 2003, Lect. Notes in Phys., 614, 155
Duric, N., & Seaquist, E. R. 1986, ApJ, 301, 308
Fenech, D. M., Muxlow, T. W. B., Beswick, R. J., Pedlar, A., & Argo, M. K. 2008, MNRAS, 391, 1384
Freedman, W. L., Madore, B. F., Gibson, B. K., et al. 2001, ApJ, 553, 47
Gordon, S. M., Kirshner, R. P., Long, K. S., et al. 1998, ApJS, 117, 89
Gordon, S. M., Duric, N., Kirshner, R. P., Goss, W. M., & Viallefond, F. 1999, ApJS, 120, 247
Green, D. A. 1984, MNRAS, 209, 449
Green, D. A. 2005, Mem. SAIt, 76, 534
Green, D. A. 2009, Bull. Astron. Soc. India, 37, 45
Hilditch, R. W., Howarth, I. D., & Harries, T. J. 2005, MNRAS, 357, 304
Kesteven, M. J. L. 1968, Aust. J. Phys., 21, 739
Kronberg, P. K., Biermann, P., & Schwab, F. R. 1985, ApJ, 291, 693
Kronberg, P. K., Sramek, R. A., Birk, G. T., et al. 2000, ApJ, 535, 706
Long, K. S. 1983, in SNRs and their X-ray emission, ed. J. Danziger, & P. Gorenstein, Reidel, 583
Macri, L. M., Stanek, K. Z., Bersier, D., Greenhill, L. J., & Reid, M. J. 2006, ApJ, 652, 113
Mathewson, D. S., Ford, V. L., Dopita, M. A., et al. 1984, ApJS, 55, 189
McKee, C. F., & Ostriker, J. P. 1977, ApJ, 218, 148
Mills, B. Y., Turtle, A. J., Little, A. G., & Durdin, J. M. 1984, Aust. J. Phys., 37, 321
Milne, D. K. 1979, Aust. J. Phys., 32, 83
Muxlow, T. W. B., Pedlar, A., Wilkinson, P. N., et al. 1994, MNRAS, 266, 455
Pietsch, W., Misanovic, Z., Haberl, F., et al. 2004, A&A, 426, 11
Plucinsky, P. P., Williams, B., Long, K. S., et al. 2008, ApJS, 174, 366
Poveda, A., Woltjer, L. 1968, AJ, 73, 65
Seaquist, E. R., & Stankovic, M. 2007, ApJ, 659, 347
Truelove, J. K., & McKee, C. F. 1999, ApJS, 120, 299
Shklovsky, I. S. 1960, Sov. Astron., 4, 243
Urošević, D., Pannuti, T. G., Duric, N., & Theodorou, A. 2005, A&A, 435, 437
van der Laan, H. 1962, MNRAS, 124, 125